The International Journal of Advanced Manufacturing Technology (2022) 118:2993–3003
https://doi.org/10.1007/s00170-021-08131-x

ORIGINAL ARTICLE

3D printing of high-strength water-soluble salt cores via material extrusion

Xiaolong Gong[1] · Xinwang Liu[1] · Zheng Chen[1] · Zhiyuan Yang[1] · Wenming Jiang[1] · Zitian Fan[1]

Received: 23 May 2021 / Accepted: 27 September 2021 / Published online: 8 October 2021

Abstract

Core materials with high strength and excellent collapsibility are important for the manufacture of hollow composite structure castings. In this work, a novel technology to fabricate water-soluble Na_2SO_4-NaCl-based salt cores with high strength and low cost by material extrusion (ME) was reported. The water-soluble Na_2SO_4 and NaCl powders were used as the matrix materials, and the bauxite powder was used as the reinforcing material. The effects of bauxite powder content and liquid phase sintering parameters on the properties of the salt cores were studied. The results show that the salt-based slurry exhibits shear thinning property within the studied bauxite powder contents. When the content of bauxite powder was 20 wt.% and the sintering was at 630 ℃/30 min, the obtained salt cores show an optimal comprehensive performance, with the bending strength, linear shrinkage, water solubility rate, and moisture rate of 24.43 MPa, 6.3%, 207.6 (g/min·m^2), and 0.29%, respectively. The complex water-soluble salt core samples prepared under optimal parameters display high-strength and well-shaped morphology.

Keywords Additive manufacturing · Material extrusion · Water-soluble salt cores · Bauxite powder · Reinforcement

1 Introduction

With the rapid development of aerospace, automotive, and communications industries, light alloy castings, such as aluminum, and magnesium alloy die castings have been widely used in these fields [1–3]. However, in order to further pursue the structural rationality and lightweight of the key parts, the light alloy die castings tend to be integrated and complicated, resulting in more complex internal cavity channels inside the castings, which put forwards higher requirements for the core materials used to form complex hollow structure castings [4–6]. Normally, the sand cores cannot meet the conditions of industrial applications due to their lower strength and poor collapsibility, while the ceramic cores have poor collapsibility in spite of sufficient strength [7–11].

The water-soluble salt cores have attracted considerable attention due to their excellent properties including high strength, low gas evolution, and good water-soluble collapsibility, which are desired for the preparation of complex hollow composite structure castings [12–15]. Liu and Gong et al. [16, 17] prepared KNO_3-based water-soluble salt cores with bending strength of 42–46 MPa for zinc alloy die castings by gravity casting method. Yaokawa et al. [13] fabricated salt cores composed of alkali carbonate and alkali chloride with bending strength of 20–30 MPa for aluminum alloy die castings by gravity casting method. Jelínek et al. [18] reported NaCl and KCl salt cores with bending strength of 5.3–10 MPa through squeezing technology using alkali silicates as a binder. Sakoda et al. [19] prepared NaCl and KCl salt cores with bending strength of 20–37 MPa for aluminum alloy die castings by pressing sintering method. Among all these researches, the bending strength of the salt cores fabricated by gravity casting method or pressing sintering method had exceeded 20 MPa, which can be used for the manufacture of aluminum alloy die castings. However, these traditional methods have some disadvantages, such as necessary molds, high cost, and high energy consumption. Especially, the geometric design and structural complexity of salt core products are limited by the current forming

✉ Xinwang Liu
liuxw@hust.edu.cn

✉ Zitian Fan
fanzt@hust.edu.cn

[1] State Key Laboratory of Materials Processing and Die & Mould Technology, School of Materials Science and Engineering, Huazhong University of Science and Technology, Wuhan 430074, China

processes, which seriously impedes its industrial application. Therefore, it is of great significance to explore a new forming process to prepare complex water-soluble salt cores with high strength and low cost.

Material extrusion (ME), as a kind of additive manufacturing technology, can freely form parts without molds [20, 21], which provides a new direction for the preparation of complex water-soluble salt cores with a low cost. In the ME technology, the solid powder materials are made into a uniformly dispersed slurry, and then the slurry is continuously extruded to form components under certain pressures according to the designed geometry [22, 23]. In recent years, this technology has been used to prepare high porosity structural parts and biomedical scaffolds with NaCl, $CaCl_2$, and $CuSO_4$ as the matrixes [24–26]. Due to the excellent water solubility of inorganic salt materials, all these studies have focused on the spatial network structure but ignoring improving the mechanical properties of the salt-based templates. The salt core materials and sintering process are critical to the mechanical properties of the water-soluble salt core. However, there are few reports on the preparation of high-strength water-soluble salt cores through the ME method.

In this paper, a novel method was developed to fabricate high-strength salt cores by material extrusion process using Na_2SO_4 powder and NaCl powder as the matrix material, and the bauxite powder was selected as the reinforcing material. The effects of bauxite powder content and liquid phase sintering parameters on the bending strength, linear shrinkage, water solubility, and porosity of the salt cores were investigated. The optimized process parameters were obtained. Finally, the complex water-soluble salt core components with high strength were prepared under optimized experimental conditions. This method provides a new way to obtain complex water-soluble salt cores with high strength and low cost, which has important theoretical and practical significance for the water-soluble salt cores in industrial development.

2 Materials and methods

2.1 Raw materials

In this study, water-soluble sodium sulfate powder (Na_2SO_4, 95 wt.% purity, D_{50} = 12.5 μm) and sodium chloride powder (NaCl, 99 wt.% purity, D_{50} = 75 μm) were selected as the matrix materials. Bauxite powder (D_{50} = 45 μm, Zhengzhou Xiangyu Casting Material Co., Ltd., China) was selected as the reinforcing material. Anhydrous ethanol (EtOH) (analytical purity, Sinopharm Chemical Reagent Co., Ltd., China) was adopted as a carrier liquid for preparing the salt-based slurry. Polyvinyl pyrrolidone (PVP) (Shandong Yousuo Chemical Technology Co., Ltd., China) was used as a binder, and methyl silicone oil was used as a release agent. The compositions of the salt-based slurry are listed in Table 1, and the mole percentage of Na_2SO_4 and NaCl is 30:70 mol%.

2.2 Preparation process

Figure 1 depicts the schematic diagram of preparing water-soluble salt cores via ME technology. The preparation process of the salt cores mainly includes salt-based slurry preparation, extrusion forming, and sintering. The solid powder (Na_2SO_4, NaCl, and bauxite) was first added to an anhydrous ethanol solution with 15 wt.% PVP and stirred manually, and then ball milling was carried out in a planetary mixer for 8 h at 180 rpm to obtain a stable salt-based slurry. To follow, the salt-based slurry was transferred to an extrusion device made by our research group, which is modified from a dispenser machine and driven by air pressure. The salt-based slurry was extruded according to the designed route by pneumatic actuation to form the required samples at room temperature, and the printing parameters of the ME technology are shown in Table 2. Finally, the salt core green body was dried in drying oven at 50 ℃ for 8 h, and the dried green body was sintered at the set temperature to obtain salt core samples.

Table 1 Compositions of the salt-based slurry

Liquid component		Solid powder			Proportion of bauxite in solid powder (wt.%)
EtOH (g)	PVP (g)	Na_2SO_4 (g)	NaCl (g)	Bauxite (g)	
20.4	3.6	38.75	37.25	0	0
		36.81	35.39	3.8	5
		34.88	33.52	7.6	10
		31.0	29.80	15.2	20
		27.13	26.07	22.8	30

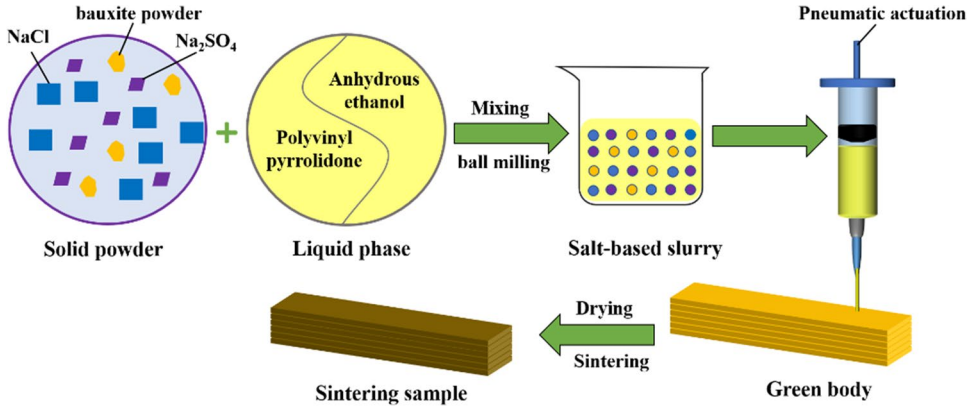

Fig. 1 Schematic diagram of the ME technology to prepare water-soluble salt cores

Table 2 Printing parameters for salt-based slurry

Printing parameters	Values
Nozzle diameter	0.41 mm
Layer height	0.38 mm
Printing speed	20 mm/s
Air pressure	0–2 kg/cm^2

2.3 Measurement and characterization

A stress-controlled rheometer (DHR-2, TA, USA) was used to test the rheological behaviors of the salt-based slurry with a parallel plate of 25 mm in diameter and a testing gap of 1000 μm. An ElectroPuls all-electric dynamic and fatigue test system (ElectroPuls E1000, Instron, USA) was used to measure the bending strength of the salt cores using a three-point-bending method with a span of 30 mm and a pressure head loading speed of 0.5 mm/min, and five samples (50 × 7 × 7 mm in length, width, and height, respectively) were measured in each group to reduce the error. The water solubility rate (K) of the salt cores was calculated by Eq. (1):

$$K = \frac{m}{s \times t} \tag{1}$$

where m and s represent the mass and total surface area of the salt core samples, respectively, and t is the dissolution time of the salt core samples in still water at 40 ℃. The linear shrinkage (L) of the salt core samples was measured according to Eq. (2):

$$L = \frac{l_1 - l_2}{l_1} \times 100\% \tag{2}$$

where l_1 and l_2 represent the length of dried samples and sintered samples, respectively. The moisture rate (φ) of the salt core samples was calculated according to Eq. (3):

$$\varphi = \frac{m_1 - m_0}{m_0} \times 100\% \tag{3}$$

where m_0 represents the original mass of the salt core samples and m_1 represents the mass of the salt core samples exposed to the air (relative humidity, 60–70%) for 2 days. The bulk density (D_b), open porosity (P_o), and closed porosity (P_c) of the salt core samples were tested using the Archimedes method with the equations, respectively, displayed in Eqs. (4) and (5) [27]:

$$P_o = \frac{M_1 - M_0}{M_1 - M_2} \times 100\% \tag{4}$$

$$P_c = \frac{M_0 - M_2 - M_o \times \rho_0/\rho_r}{M_1 - M_2} \times 100\% \tag{5}$$

where M_0 represents the mass of dried salt core samples, M_1 is the mass of kerosene-saturated salt core samples in air, and M_2 is the mass of samples in kerosene. ρ_0 is the density of kerosene (0.8 g/cm^3), and ρ_r is the real density of the salt core samples. Five tests were performed for each material state to ensure good reproducibility.

Thermogravimetric and differential thermal analysis (TG–DTA, PerkinElmer Instruments) were performed on the green body after drying to determine the sintering process, and the heating temperature was increased from room temperature to 640 °C at a rate of 10 °C/min. The compositions of the salt core samples were analyzed using X-ray diffraction (XRD-7000S, Japan) with a Cu Kα radiation. The micromorphology of the salt core samples pretreated by carbon sputtering was observed using a scanning electron microscope (SEM, Quanta 200) equipped with an energy dispersive spectrometer (EDS).

3 Results and discussion

3.1 Material extrusion of salt cores

Rheological properties of the salt-based slurry are critical to fabricate the salt cores using a ME method, and the rheological behaviors of salt-based slurry with different bauxite powder contents are shown in Fig. 2. It can be observed that the salt-based slurry with different bauxite powder contents exhibits shear thinning property, which means that the salt-based slurry can be extruded smoothly from the nozzle, and the extruded slurry will be rapidly deposited and formed without shear force. Meanwhile, it can also be seen that the viscosity and shear stress of the slurry decrease as the content of bauxite powder increases. The reason is that the density of bauxite powder (3.45 g/cm^3) is greater than that of NaCl (2.16 g/cm^3) and Na_2SO_4 (2.68 g/cm^3). Increasing of bauxite powder content, the volume fraction of the solid powder (Na_2SO_4, NaCl, and bauxite) decreases, leading to the decrease of the solid content of the salt-based slurry.

The salt core green body prepared by ME technology was then sintered in order to obtain excellent mechanical property. The sintering process of the salt core green body was determined by the TG–DTA results, as shown in Fig. 3. It can be seen from Fig. 3a that the PVP in salt core green body is decomposed at about 350 ℃, and with the further increase of temperature, the salt core green body begins to melt at about 620 ℃, which is in good agreement with the solidus temperature of NaCl-Na_2CO_3 binary phase diagram [28]. The liquid phase sintering temperature was set to 630 ℃ based on our previous experiments. Therefore, the sintering process of the salt core green body was carried out according to Fig. 3b. First, the salt core green body was calcined at 350 ℃ for 1 h with a heating rate of 1 ℃/min to remove the PVP organic matter and then elevated the temperature to 600 ℃ at a heating rate of 3 ℃/min, and the temperature was kept for 60 min to ensure the same temperature inside and outside the salt cores. Finally, it was heated to 630 ℃ and kept for 15 min, 30 min, and 45 min, respectively, to complete the liquid phase sintering and obtain the salt core samples.

3.2 Performance characteristics

Figure 4 shows the effects of bauxite powder content at various sintering time on bending strength and linear shrinkage of the salt core samples. It is evident that the bauxite powder content and sintering time have a remarkable influence on

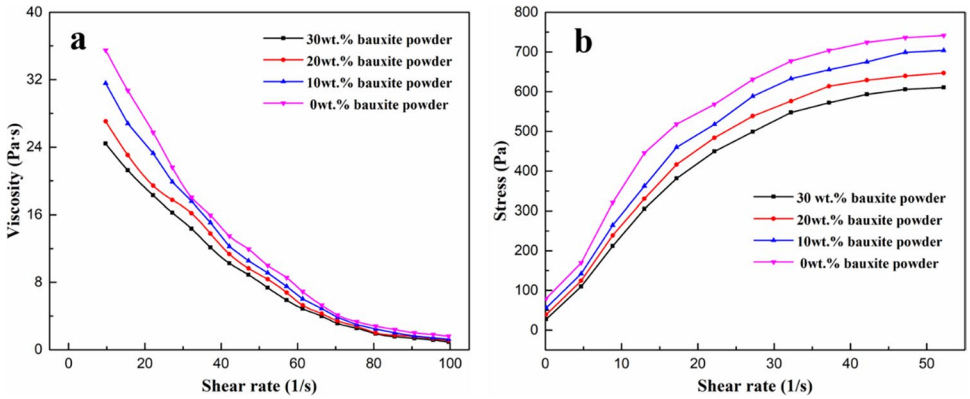

Fig. 2 Rheological behaviors of salt-based slurry with different bauxite powder contents: **a** viscosity versus shear rate and **b** stress versus shear rate

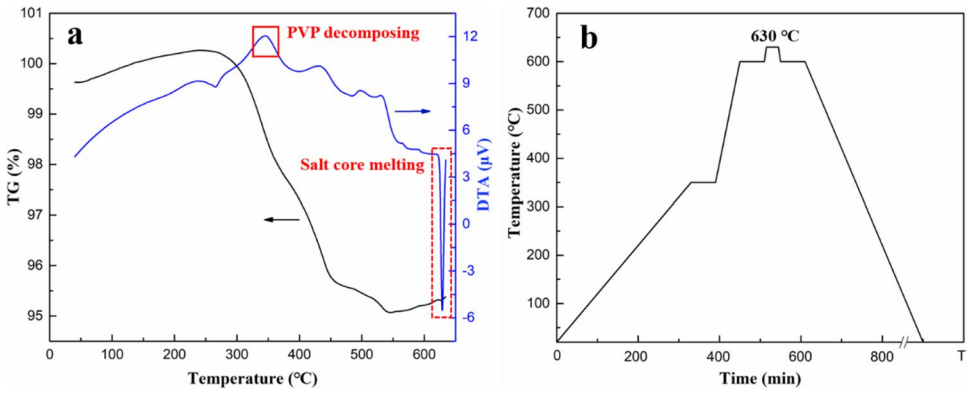

Fig. 3 Sintering process of salt core green body: **a** TG–DTA curves and **b** sintering temperature versus sintering time

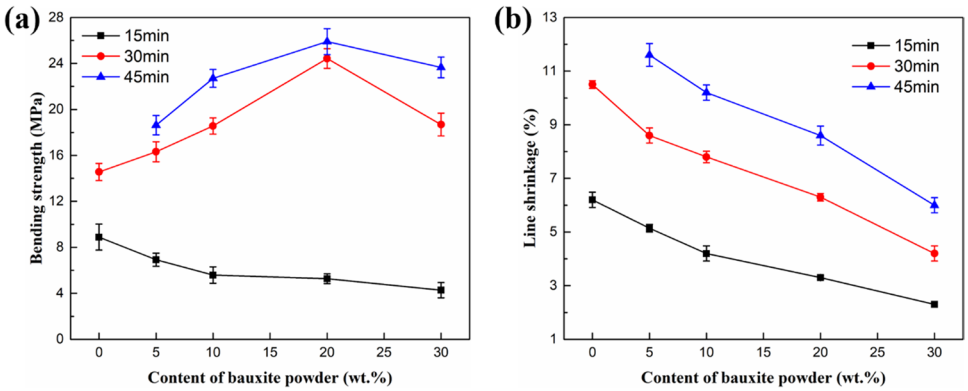

Fig. 4 Effects of bauxite powder content at various sintering times on the salt core samples: **a** bending strength and **b** linear shrinkage

the bending strength and linear shrinkage of the salt core. As illustrated in Fig. 4a, when the sintering time is 15 min, the bending strength of the salt core is less than 9 MPa, and the bending strength decreases with the increase of bauxite powder content. When the sintering time is 30 min and 45 min, respectively, the bending strength of the salt core increases first and then decreases as the content of bauxite powder increases. For example, when the sintering time is 30 min, the bending strength of the salt core increases dramatically from 14.56 to 24.43 MPa with increasing the bauxite powder content from 0 to 20 wt.% and then decreases to 18.68 MPa as the bauxite powder content further increase to 30 wt.%. It should be noted that the salt core samples without bauxite powder (0 wt.%) are destroyed by excessive melting when the sintering time is 45 min.

As illustrated in Fig. 4b, when the sintering time is constant, the linear shrinkage of the salt core decreases with the increase of bauxite powder content. When the content of bauxite powder is constant, the linear shrinkage increases with the increase of sintering time. For example, when the sintering time is 30 min, with the content of bauxite powder increasing from 0 to 30 wt.%, the linear shrinkage decreases from 10.5 to 4.2%. It is well-known that the bending strength and linear shrinkage are the main properties of the salt core. First, the salt core is a brittle material and needs high strength to resist the impact of liquid metal during high-pressure die casting. Second, low shrinkage is necessary to ensure the precision of castings.

Figure 5 shows the effects of bauxite powder content at various sintering times on open porosity and close porosity of the salt core samples. As can be seen, the open porosity decreases with the increase of sintering time, while the close porosity shows the opposite trend. When the content of bauxite powder is 20 wt.%, the open porosity decreases dramatically from 21.97 to 3.08% with increasing the sintering time from 15 to 45 min, while the closed porosity increases from 4.5 to 9.58%. When the sintering time is 15 min, the salt core possesses a higher open porosity and a lower closed porosity, which is caused by insufficient sintering time. When the sintering time is 30 min and 45 min, respectively, the open porosity increases slowly and then sharply with the increase of bauxite powder content. Such phenomenon might result from two factors. On the one hand, the bauxite powder is a refractory material that will improve the thermal stability of the salt core. On the other hand, the excessive bauxite powder is prone to agglomeration and would reduce the fluidity of the liquid phase [29].

Figure 6 depicts the effects of bauxite powder content at various sintering times on water solubility rate and moisture rate of the salt core samples. As shown in Fig. 6, the water

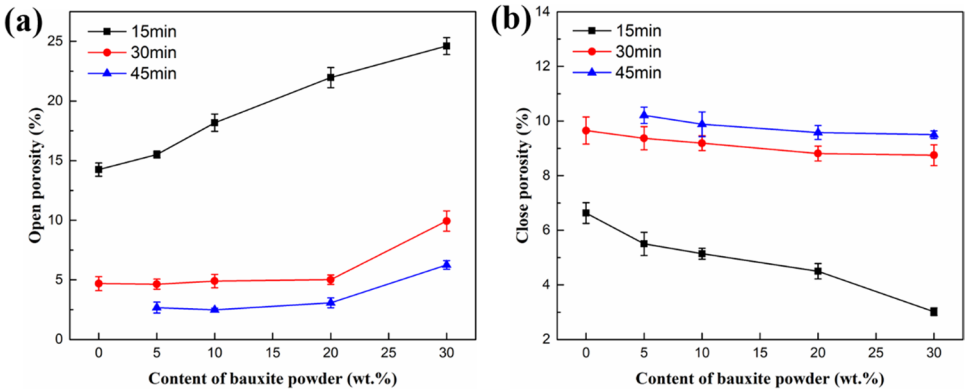

Fig. 5 Effects of bauxite powder content at various sintering times on the salt core samples: **a** open porosity and **b** close porosity

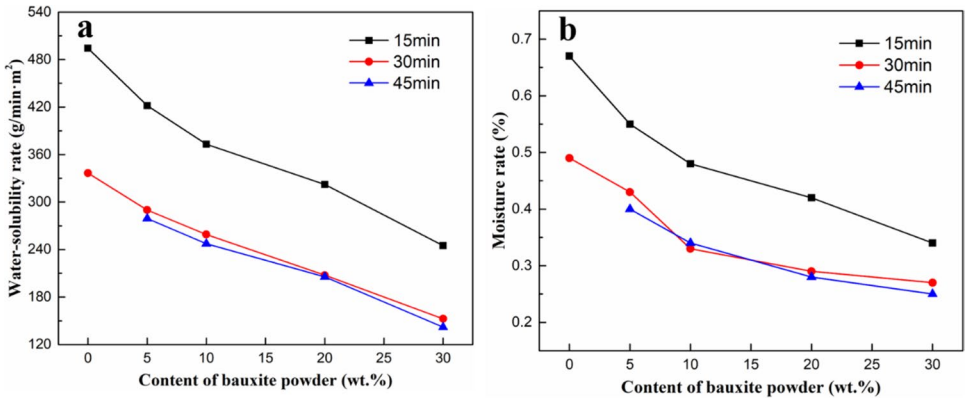

Fig. 6 Effects of bauxite powder content at various sintering times on the salt core samples: **a** water solubility rate and **b** moisture rate

solubility rate and the moisture rate display an overall trend of decreasing with the increase of sintering time and bauxite powder content, respectively. When the sintering time is 30 min, as the bauxite powder content increases from 0 to 30 wt.%, the water solubility rate of the salt core decreases from 336.7 to 152.6 (g/min·m^2), and the moisture rate decreases from 0.49 to 0.27%. When the content of bauxite powder is 20 wt.%, with the increases of sintering time from 15 to 45 min, the water solubility rate and the moisture rate of salt core decrease from 322.1 (g/min·m^2) to 205.4 (g/min·m^2) and from 0.42% to 0.28%, respectively. For the water-soluble salt core, the higher water solubility rate is beneficial to the removal from the castings, and the lower moisture rate is conducive to the storage of the salt core. Generally, the higher the densification degree of the salt core, the lower its water solubility rate and moisture rate. Furthermore, the bauxite powder as an insoluble material can also reduce the water solubility rate and moisture rate of the salt core.

In conclusion, when the sintering time and the bauxite powder content are 30 min and 20 wt.%, respectively, the obtained salt core samples possess excellent comprehensive properties, which the bending strength, linear shrinkage rate, water solubility rate, and moisture rate are 24.43 MPa, 6.3%, 207.6 (g/min·m^2), and 0.29%, respectively.

3.3 Microstructure analysis

Figure 7 shows the XRD patterns of the salt core samples with different bauxite powder contents sintered for 30 min. It can be observed that the salt cores are mainly composed of NaCl phase, Na_2SO_4 phase, and Al_2O_3 phase, and there is no other new phase detected, which indicates that the bauxite powder has not reacted with the salt melt and stably exists in the salt core matrix.

Figure 8 shows the EDS map analyses of the salt core samples with 20 wt.% bauxite powder at 30-min sintering. It can be seen that the elements of Na, Cl, Al, S, and O are clearly distributed in the salt core, and the NaCl (Cl element) and bauxite powders (Al element) are relatively dispersed in the salt core. Furthermore, it can also be observed that the bauxite powder is distributed around the NaCl phase.

Figure 9 shows the microstructures of the salt core samples with 20 wt.% bauxite powder at different sintering times. When the sintering time is 15 min, as shown in Fig. 9a and d, a large number of open pores are visible, and only a small amount of solid powder was sintered into agglomerates. When the sintering time is 30 min, as shown in Fig. 9b and e, the pores of the salt core remarkably reduce, and the densification degree increases. In addition, some closed pores are observed in the salt core. As the sintering time increases to 45 min, the densification degree of salt core is further improved, as shown in Fig. 9c and f. This is because increasing the sintering time can increase the liquid phase volume, thereby enhancing the efficiency of particle rearrangement and mass transfer. However, the shrinkage will be generated during the solidification of the liquid phase, resulting in some closed pores in the salt core, most of which are spherical or nearly spherical.

Generally, ceramic powder as a reinforcing material can improve the solidification structure of the salt cores [16, 29]. The microstructures of the salt core samples with different bauxite powder contents at 30-min sintering are shown in Fig. 10, and Table 3 lists the EDS results of the salt cores selected in Fig. 10. According to the results of EDS analysis, it suggests that the components of the salt core are NaCl, Na_2SO_4, and bauxite powder, which matches the results of XRD and EDS map analyses. It can be seen from Fig. 10a–d that the NaCl phase is significantly refined with the increase of bauxite powder content, and the NaCl phase changes from coarse lath crystals to fine bulk crystals gradually. The grain refinement can promote the strength of the salt core, which can be explained by the Hall–Petch Eq. (6) [30], where σ represents the yield strength of the salt cores, D represents the mean grain size, σ_0 is the intrinsic yield strength, and K is the material constant.

$$\sigma = \sigma_0 + KD^{-1/2} \tag{6}$$

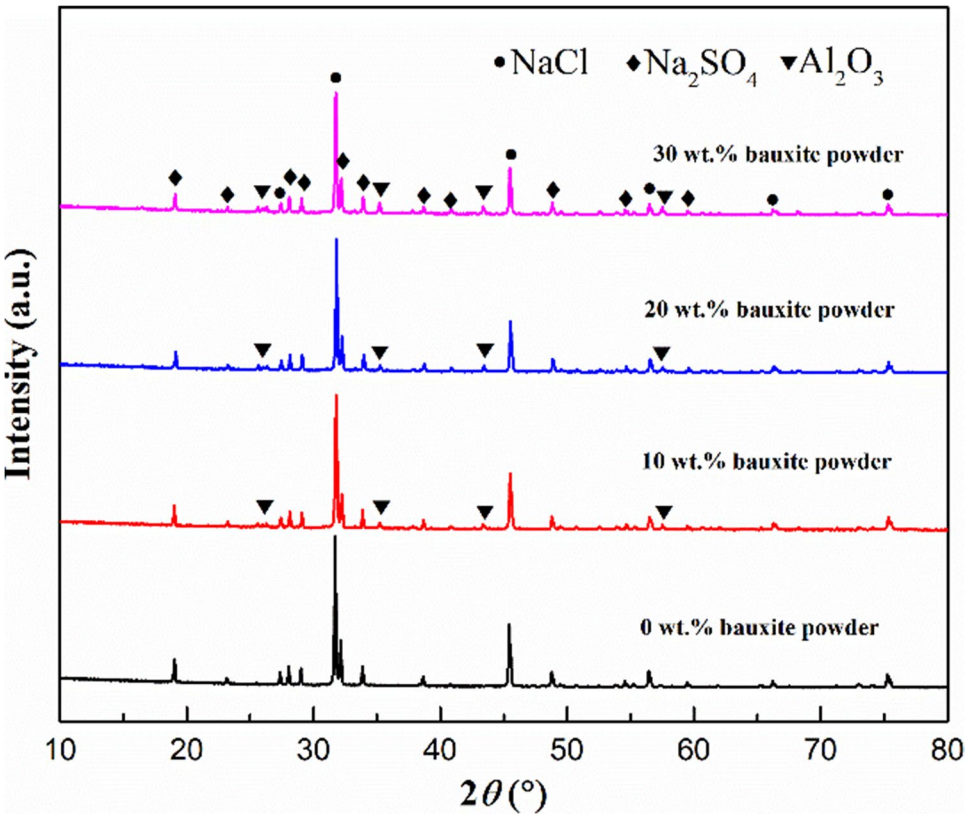

Fig. 7 XRD pattern of the salt core with different bauxite powder contents sintered for 30 min

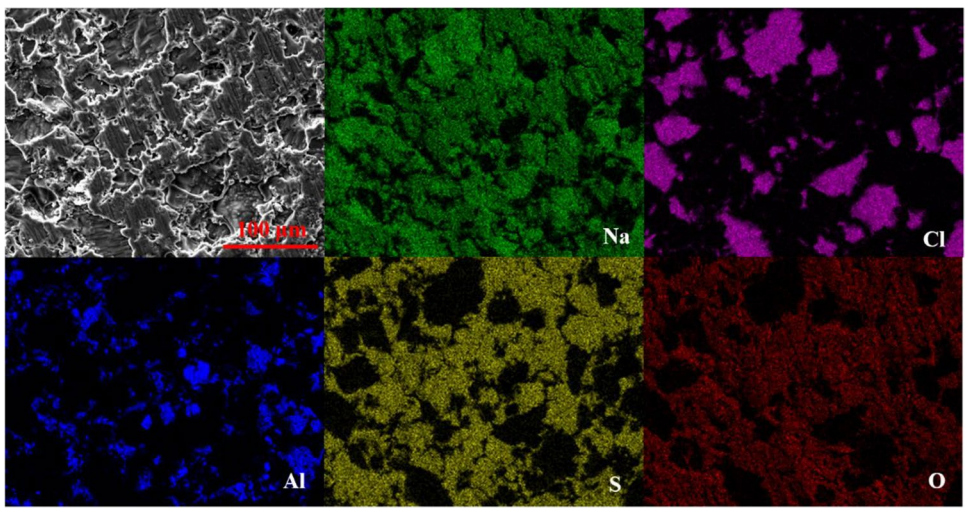

Fig. 8 EDS map analyses of salt core samples with 20 wt.% bauxite powder sintered for 30 min

The appropriate ceramic powder can improve the performance of the salt core, but excessive addition may have the opposite effect [29, 31]. Many defects were observed when the bauxite powder content is 30 wt.%, as shown in Fig. 11, resulting in a decrease in the bending strength of the salt core.

Figure 12 depicts the images of the salt core samples with 20 wt.% bauxite powder under different sintering times. The side profile of the salt core samples is displayed in Fig. 12a–d, and the cross-section profile of the salt core samples is displayed in Fig. 12e–h. It is clear that the deformation degree of salt core increases with prolonging the sintering time. When the sintering time is 45 min, the salt core has a serious bending deformation, as shown in Fig. 12d and h. Therefore, the sintering time of 30 min is the relatively optimal parameter.

The complex salt core samples were prepared using the optimized parameters, and the bauxite powder content and sintering time are 20 wt.% and 30 min, respectively, as shown in Fig. 13. It can be seen that the salt core samples

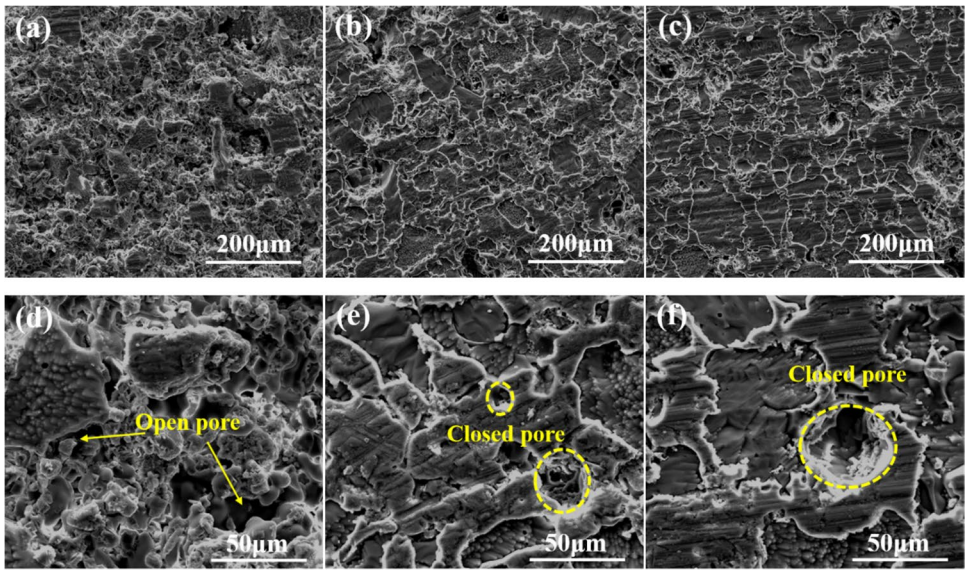

Fig. 9 Microstructures of salt core samples with 20 wt.% bauxite powder at different sintering times: **a**, **d** 15 min; **b**, **e** 30 min; and **c**, **f** 45 min

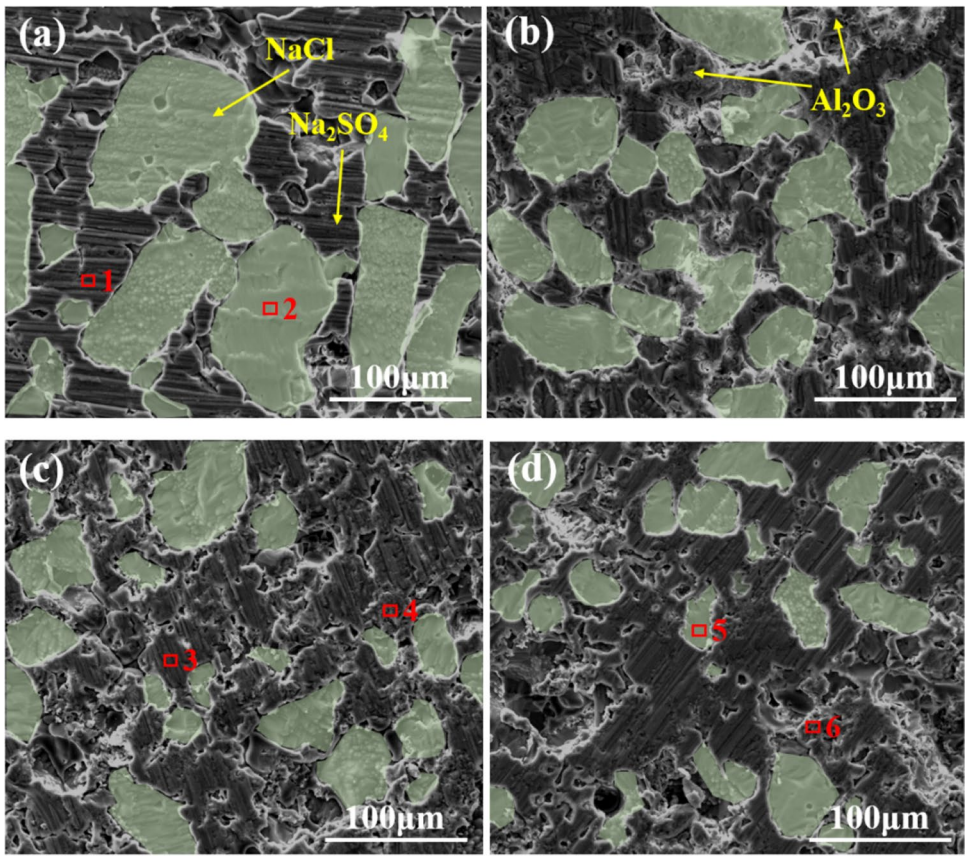

Fig. 10 Microstructures of salt core samples with different bauxite powder contents sintered for 30 min: **a** 0 wt.%; **b** 10 wt.%; **c** 20 wt.%; and **d** 30 wt.%

after sintering have no obvious deformation, and no other defects are presented, indicating that it is feasible to manufacture a complex high-strength water-soluble salt core via ME technology.

Table 3 EDS results of the selected positions of the salt core samples corresponding to Fig. 10

Area No	Element compositions (at.%)					Component
	O	Na	Al	S	Cl	
1	36.37	32.93	-	30.7	-	Na_2SO_4
2	-	47.16	-	-	52.84	NaCl
3	37.63	33.74	-	28.63	-	Na_2SO_4
4	52.54	-	47.46	-	-	Al_2O_3
5	-	46.41	-	-	53.59	NaCl
6	58.78	-	41.22	-	-	Al_2O_3

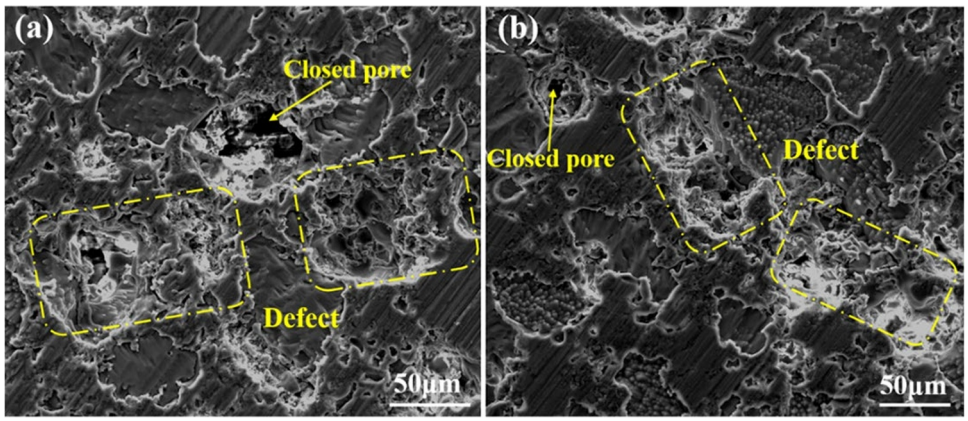

Fig. 11 Microstructures of salt core samples with 30 wt.% bauxite powder at different sintering times: **a** 30 min and **b** 45 min

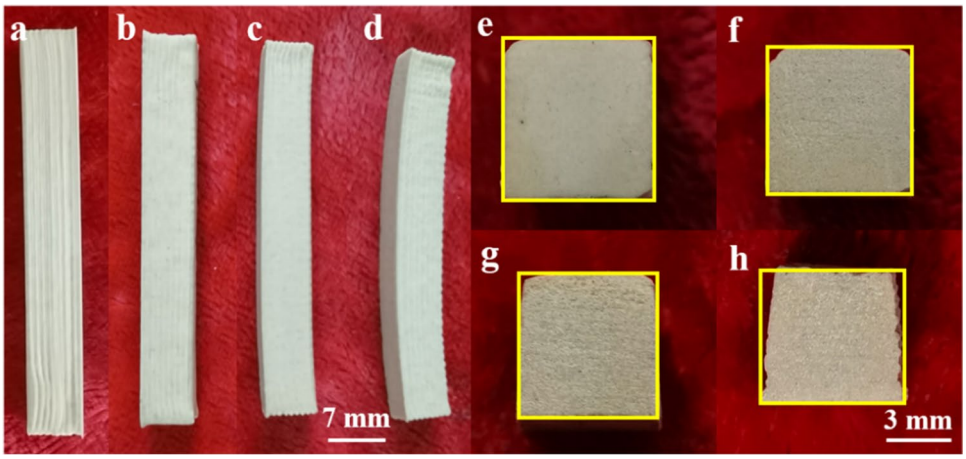

Fig. 12 Images of the salt core samples with 20 wt.% bauxite powder under different sintering times: **a**, **e** 0 min (green body); **b**, **f** 15 min; **c**, **g** 30 min; and **d**, **h** 45 min

4 Conclusion

In this paper, we utilized the material extrusion (ME) method to prepare water-soluble salt core strengthening by bauxite powder. The bauxite powder content and sintering parameters have a significant effect on the performance of the salt cores. Increasing the content of bauxite powder is beneficial to refine the NaCl phase, and prolonging the sintering time facilitates the densification of the salt core. However, excessive bauxite powder and longtime sintering are not conducive to the formation of the salt cores. The salt cores with 20 wt.% bauxite powder sintered for 30 min at 630 ℃ possess an excellent comprehensive performance, which satisfies the requirements for manufacturing hollow composite structure castings. The complex water-soluble high-strength salt core samples with high-strength and well-shaped morphology are successfully fabricated under optimal parameters, indicating the ME is promising in the preparation of water-soluble salt cores.

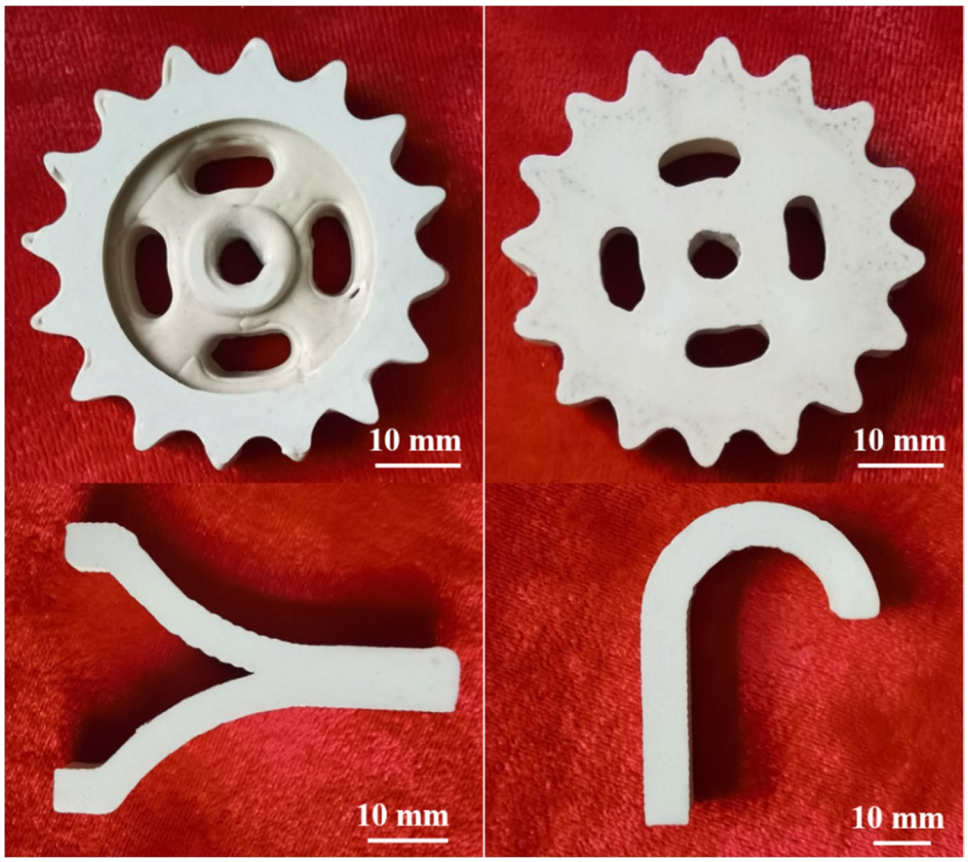

Fig. 13 Images of complex salt core samples fabricated by material extrusion with optimal parameters

Author contribution Xiaolong Gong and Xinwang Liu designed and participated in experiments and wrote the manuscript draft. Zheng Chen and Zhiyuan Yang performed the experiments. Wenming Jiang analyzed the data. Zitian Fan directed this study, revised the manuscript, and provided the funding. All the authors read and approved the final manuscript.

Funding The authors would like to thank the support of the National Natural Science Foundation of China (No. 51775204 and 51971099) and the Analytical and Testing Center, HUST.

Availability of data and materials The data used to support the findings of this study are included within the article.

Declarations

Ethics approval Not applicable.

Consent to participate Not applicable.

Consent for publication Not applicable.

Competing interests The authors declare no competing interests.

References

1. Dong X, Yang H, Zhu X, Ji S (2019) High strength and ductility aluminium alloy processed by high pressure die casting. J Alloy Compd 773:86–96
2. Benedyk JC (2010) Aluminum alloys for lightweight automotive structures. Illinois Institute of Technology Press, USA
3. Alam T, Ansari AH (2017) Review on aluminium and its alloys for automotive applications. Int J Adv Technol Eng Sci 5:278–294
4. Wang T, Zha J, Jia Q, Chen Y (2016) Application of low-melting alloy in the fixture for machining aeronautical thin-walled component. Int J Adv Manuf Technol 87:2797–2807
5. Luo AA, Sachdev AK, Powell BR (2010) Advanced casting technologies for lightweight automotive applications. China Foundry 7:463–469
6. Kallien L, Weidler T, Becker M (2014) Production of magnesium die castings with hollow structures using gas injection technology in the hot chamber die casting process. Int Foundry Res 66:05–07
7. Jiang P, Liu FC, Fan ZT, Jiang WM, Liu XW (2016) Performance of water-soluble composite sulfate sand core for magnesium alloy castings. Arch Civ Mech Eng 14:494–502
8. Stauder BJ, Kerber H, Schumacher P (2016) Foundry sand core property assessment by 3-point bending test evaluation. J Mater Process Technol 237:188–196
9. Liu FC, Yang L, Huang Y, Jiang P, Li G, Jiang WM, Fan ZT (2017) Performance of resin bonded sand for magnesium alloy casting. J Manuf Process 30:313–319
10. Cho GH, Li J, Kim EH, Jung YG (2015) Preparation of a ceramic core with high strength using an inorganic precursor and the gel-casting method. Surf Coat Technol 284:396–399

11. Ke R, Dong Y (2021) Preparation and properties of water-soluble ceramic core for light alloy investment casting. Mater Today Commun 26:101918
12. Xiao Z, Harper LT, Kennedy AR, Warrior NA (2017) A water-soluble core material for manufacturing hollow composite sections. Compos Struct 182:380–390
13. Yaokawa J, Miura D, Anzai K, Yamada Y, Yoshii H (2007) Strength of salt core composed of alkali carbonate and alkali chloride mixtures made by casting technique. Mater Trans 48:1034–1041
14. Beňo J, Adámková E, Mikšovský F, Jelínek P (2015) Development of composite salt cores for foundry applications. Mater Technol 49:619–623
15. Jiang W, Dong J, Lou L, Liu M, Hu Z (2010) Preparation and properties of a novel water soluble core material. J Mater Sci Technol 26:270–275
16. Liu FC, Tu S, Gong XL, Li GJ, Fan ZT (2020) Comparative study on performance and microstructure of composite water-soluble salt core material for manufacturing hollow zinc alloy castings. Mater Chem Phys 252:123257
17. Gong XL, Jiang WM, Liu FC, Yang ZY, Guan F, Fan ZT (2021) Effects of glass fiber size and content on microstructures and properties of KNO_3-based water-soluble salt core for high pressure die casting. Int J Metalcast 15:520–529
18. Jelínek P, Adámková E (2014) Lost cores for high-pressure die casting. Arch Foundry Eng 14:101–104
19. Sakoda T, Suzuki T (1976) Water soluble core for pressure die casting and process for making the same. US3963818A
20. Compton BG, Lewis JA (2015) 3D-printing of lightweight cellular composites. Adv Mater 26:5930–5935
21. Tang SY, Yang L, Li GJ, Liu XW, Fan ZT (2019) 3D printing of highly-loaded slurries via layered extrusion forming: parameters optimization and control. Addit Manuf 28:546–553
22. Li GJ, Tang SY, Yang L, Qian L, Jiang WM, Fan ZT (2019) Fabrication of soluble salt-based support for suspended ceramic structure by layered extrusion forming method. Mater Des 183:108173
23. Tang SY, Fan ZT, Zhao HP, Yang L, Liu FC, Liu XW (2018) Layered extrusion forming—a simple and green method for rapid prototyping ceramic core. Int J Adv Manuf Technol 96:3809–3819
24. Zhang YM, Shao HP, Lin T, Peng J, Wang AY, Zhang ZN, Wang LH (2019) Effect of Ca/P ratios on porous calcium phosphate salt bioceramic scaffolds for bone engineering by 3D gel-printing method. Ceram Int 45:20493–20500
25. Kleger N, Cihova M, Masania K, Studart AR, Lffler JF (2019) 3D printing of salt as a template for magnesium with structured porosity. Adv Mater 31:1903783
26. Jakus AE, Geisendorfer NR, Lewis PL, Shah RN (2018) 3D-printing porosity: a new approach to creating elevated porosity materials and structures. Acta Biomater 72:94–109
27. Qian L, Yang L, Li G, Jiang WM, Fan ZT (2020) Effect of nano-TiO_2 on properties of 3 mol% yttria-stabilized zirconia ceramic via layered extrusion forming. J Eur Ceram Soc 40:4539–4546
28. https://www.crct.polymtl.ca/fact/phase_diagram.php?file=NaCl-Na2SO4.jpg&dir=FTsalt. Accessed 16 May 2020.
29. Tu S, Liu FC, Li GJ, Jiang WM, Liu XW, Fan ZT (2018) Fabrication and characterization of high-strength water-soluble composite salt core for zinc alloy die castings. Int J Adv Manuf Technol 95:505–512
30. Zhang HJ, Sun SL, Hiu HJ, Zhu Z, Wang YL (2020) Characteristic and mechanism of nugget performance evolution with rotation speed for high-rotation-speed friction stir welded 6061 aluminum alloy. J Manuf Process 60:544–552
31. Huang R, Zhang B (2017) Study on the composition and properties of salt cores for zinc alloy die casting. Inter J Metalcast 11:440–447